

Assessing hydrological response to change in climate: Statistical downscaling and hydrological modelling within the upper Nile

M. Kigobe^a, A. van Griensven^b,

^a*Department of Civil Engineering, Makerere University Kampala, Uganda, P.O Box 7062 Kampala, Uganda (mkigobe@tech.mak.ac.ug)*

^b*Department Hydroinformatics & Knowledge Management, UNESCO-IHE Institute for Water Education P.O. Box 3015, 2601 DA DELFT, The Netherlands (A.vanGriensven@unesco-ihe.org)*

Abstract: The sensitivity of several water resource components to environmental change is crucial to water managers. Water resource sensitivity studies are therefore required to assess how hydrological regimes will respond to environmental change. As a first attempt in the Upper Nile, this study explores statistical techniques to downscale climate projections with particular emphasis on rainfall simulation for the Kyoga basin, using Generalised Linear Models (GLMs). Despite noticeable bias in predicting the historical climate, the study results reveal that a warmer climate will lead to a basin-wide increase in precipitation and subsequent increase in stream flows for the Mpologoma basin, within the upper Nile.

Keywords: Climate Change, Statistical Downscaling, Hydrological Sensitivity Analysis.

1 INTRODUCTION

The Kyoga basin is located in the Upper Nile and is mainly characterised by inter-annual and inter decadal variation in precipitation. Water availability in the basin is mainly important for agriculture, fishing, municipal purposes and many other uses. Water availability is highly influenced by climate variability and climate change presents many challenges for the Nile basin and Africa in general [Conway and Hulme, 1993; Hulme, 2000; Hulme et al., 2005]. There is little doubt that climate change will alter the hydrology of the Nile basin, therefore, there is increasing interest in understanding how the rising concentration of greenhouse gases might affect climate (the mean and variability of temperature, precipitation, humidity, wind and other climate variables over several decades) at local and regional scales in the Nile basin. For the Kyoga basin, human activities in the catchment have increased over the past century and expected to grow even more rapidly in the future, hence, water management will become even more important with a changing climate. The objective of this paper is to show projections of local rainfall under different emission scenarios. This is done by means of a sensitivity approach, analyse the associated impact on selected hydrological variables for a case study of the Mpologoma basin, within the Upper Nile. The rest of the paper presents a brief description of the Mpologoma basin, a sub-catchment of the Kyoga basin in section 2, followed by the methodology in section 3 and the results and discussions in sections 4 and 5 respectively.

2 KYOGA BASIN

The Kyoga basin (Figure 1) is 51,283 km² in size and composed of several sub-basins. The biggest tributary inflow into the basin (approximately 90 % of the total inflow) is the Victoria Nile

flow, which drains into the Kyoga catchment, as a controlled release at Owen Falls dam. The average total inflow into Lake Kyoga is estimated at about $1,420 \text{ m}^3/\text{s}$, with the Victoria Nile contributing about 85 %. Other tributary flows contribute about 4 % and precipitation over the lake accounts for the remaining 11 %. The most significant tributary flow is mainly from the Mt. Elgon ranges (in the Eastern parts of the basin on the borders of Uganda and Kenya). The average annual basin precipitation is about $1,300 \text{ mm}$ and the highest precipitation falling over the Kyoga basin is received over the Elgon Mountain ranges. The Kyoga basin faces high evapotranspiration from the swamp vegetation. The Lake is not regulated and the outflow from the Kyoga basin is naturally controlled by the exit of Lake Kyoga which drains into the Kyoga Nile and later joins Lake Albert, along the Nile river system.

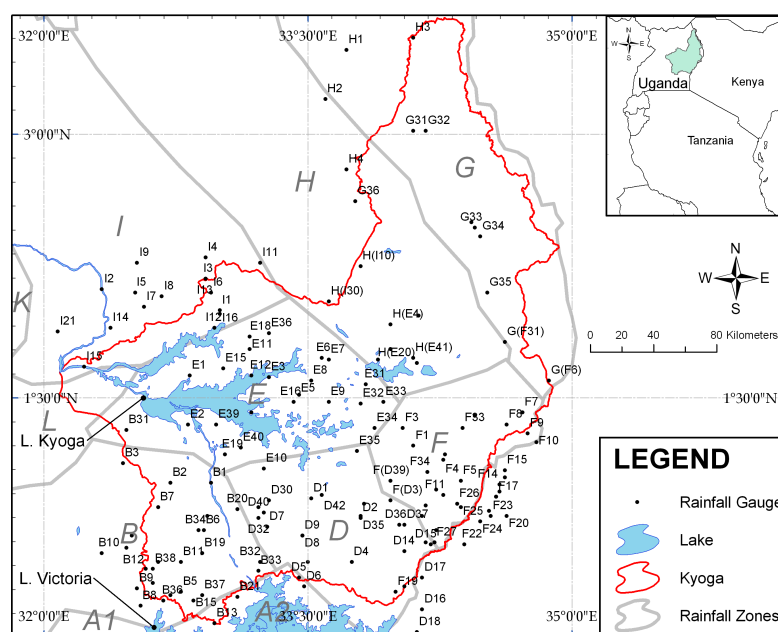


Figure 1: Precipitation gauge network for 110 rainfall sites

3 METHODOLOGY

3.1 Rainfall modelling at daily time step

A number of methods are widely reported for estimating climate change. An extensive review of the several techniques involved in representing regional and local scale processes when using climate models is given by Fowler and Kilsby [2007]. General Circulation Models (GCM) outputs, especially precipitation are not suitable for use in assessing hydrological response to climate change due to the coarse spatial resolution of the GCM outputs. To achieve better projections, one possibility is the use of precipitation outputs from Regional Climate Models (RCM). Despite the general absence of such models (RCMs) for the Kyoga basin, there are a number of other issues related to the use of RCMs for the Kyoga basin, including the requirement of large numbers of rainfall sequences. Secondly RCMs run on grid resolutions that are not adequate for local scale studies. Therefore, this study is focused on the projection of local scale rainfall at multiple sites in the Kyoga basin using statistical downscaling. Additionally, a detailed data set was available in the Kyoga basin to facilitate spatial-temporal modelling. This was done by applying the GLM models developed by Chandler and Wheater [2002]; Chandler [2006].

Generalised Linear Models (GLMs) can be regarded as multi-state Markov models which, with appropriate extensions, can include dependencies among multiple sites within a region. In the framework suggested by Stern and Coe [1984] and subsequently extended by Chandler and Wheeler [2002], the application of a GLM to daily rain gauge data involves identifying, for each day in the rainfall record, the distribution of rainfall at each site and then specifying a plausible inter-site dependence structure that preserves the single-site distributions. The distributions themselves are constructed by relating the parameters of distribution functions for rainfall occurrence and amounts to related quantities, called covariates. Typical examples of covariates include rainfall on previous days, the time of the year, the altitude of the site, and regional and global climate indices. The procedure involved is a two-step approach: (a). To model the temporal pattern of wet and dry days at a site, a logistic regression model is generally used. If P_i denotes the probability of rainfall occurrence on the i^{th} day in a dataset of rainfall, conditioned on a covariate vector x , the model is given by

$$\left[\frac{P_i}{1 - P_i} \right] = x' \beta \quad (1)$$

where β is a vector of parameters to be estimated. Any Markov chain model can be written in the form of Equation 1 by including binary covariates representing wet or dry states on previous days [Chandler, 2002]; (b). If the i^{th} day is wet then the corresponding rainfall amount is generally represented by a gamma distribution with mean μ_i , where

$$\ln(\mu_i) = \xi' \gamma \quad (2)$$

For a covariates vector ξ_i and a coefficient vector γ . The gamma distribution has a shape parameter. The shape parameter is often fixed at a constant value for each observation. Rainfall processes are commonly affected by the interacting effect of two or more covariates. For example, if the autocorrelation in rainfall amounts is, say, strongest during the rainy season, the GLM coefficient representing the effect of the previous days rainfall would vary with the seasonal covariates. In general, this kind of interaction can be incorporated by adding an additional covariate which is the product of two interacting covariates [Chandler, 2005; Yang et al., 2005]. The presence or absence of such interactions may reveal valuable information about the mechanisms driving the rainfall processes.

After GLM models are developed for a particular region, they can be extended to downscale GCM projections by means of statistical downscaling. Statistical downscaling applies empirical (statistical) relationships to bridge the large-scale features (predictors) simulated reliably by the GCMs (such as geopotential height fields, sea level pressure, humidity) and regional or local climate variables (predictands, such as temperature and precipitation at a certain location). This involves developing time-invariant relationships between large scale climate variables and local scale climate variables with the assumption that the large scale variables are reliably simulated and the relationships remain constant under a changing climate. The result from this strategy is daily simulations of rainfall at multiple sites; which can then be used to assess the impact of climate change at several sites in the Kyoga basin. The sensitivity of the basin hydrology was investigated using a distributed hydrological model which is briefly described in the following section 3.2.

3.2 Hydrological modelling on daily time step

The SWAT model was used for this study. The model is based on three major components: (i) the sub-basin itself; (ii) reservoir routing and (iii) channel routing. The sub-basin component is composed of eight modules: hydrology, weather, sedimentation, soil temperature, crop growth, nutrients, agricultural management, and pesticides. Only the hydrology and weather components are relevant to this study. The hydrology module is able to reproduce the following processes:

surface runoff, percolation, lateral subsurface flow, groundwater flow, evapotranspiration (ET) and transmission losses (Figure 2).

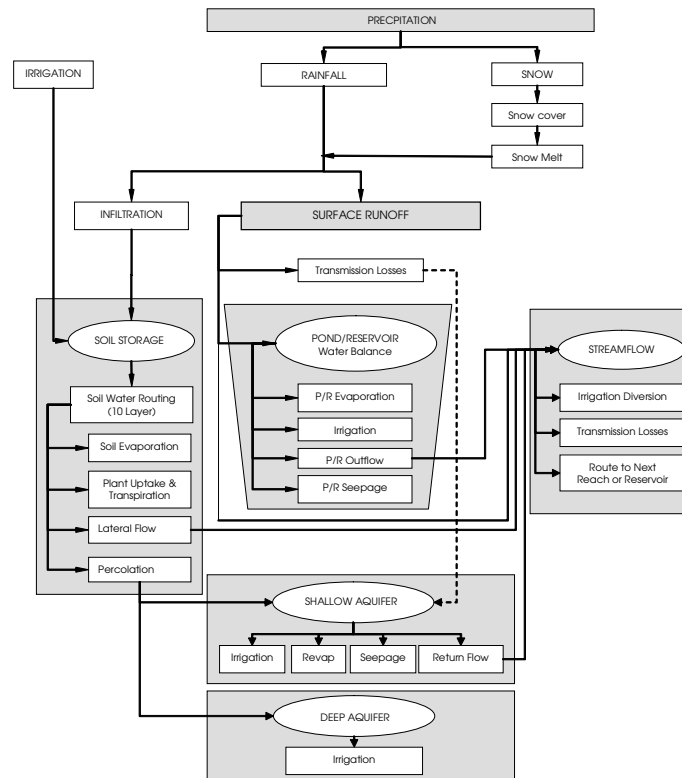


Figure 2: Schematic flow pathways for water movement in SWAT (adapted from Neitsch et al. [2000])

For this study, surface runoff was simulated based on the USDA Soil Conservation Service (SCS) Curve Number theory. The development and application of the curve number is well documented [SCS, 1972] and it is a standard hydrologic analysis technique extensively tested in the United States for small to medium sized catchments. Percolation is modelled with a layered storage routing technique combined with a crack flow model; lateral subsurface flow; groundwater flow to streams from shallow aquifers; potential evapotranspiration by the Hargreaves, PriestleyTaylor and Penman-Monteith methods; snowmelt; transmission losses from streams; and water storage and losses from ponds [Arnold et al., 1998].

The model operates at three spatial levels: basin, sub-basin and HRU. An HRU is a fraction of the sub basin that can be represented by a unique combination of soil and land use and has no physical location in the sub-basin. The program calculations follow these levels: (1) the fluxes of each HRU (per surface unit) and (2) the fluxes (outputs of previous step) are aggregated to sub-basin output, conditioned on the fractions of the HRUs, (3) the sub basin outputs are then routed through river reaches according to the river network. A detailed description of the model given by Arnold et al. [1998]; Arnold [2005] and Neitsch et al. [2000]. A detailed discussion of previous applications is given by Gassman et al. [2007].

In the Kyoga study, model calibration and uncertainty analysis, was conducted using the sequential

uncertainty fitting program SUFI-2 [Abbaspour, 2007; Abbaspour et al., 2008]. SUFI-2 is a tool for sensitivity analysis, multi-site calibration and uncertainty analysis. The tool is capable of dealing with many parameters and many variables (for example, flow, sediments, water quality, etc) for many gauging stations simultaneously and Latin Hypercubes samplings is used to draw independent parameter sets [Abbaspour, 2007].

4 RESULTS

4.1 GLM Model Structures for the Kyoga basin

The occurrence and amounts models fitted by rainfall zones were predominantly similar (Table 1), except for the additional parameter required to model the spatial correlation structures. The occurrence and amounts models fitted to the rainfall zone B are shown in Table 1. The performance of GLM models for rainfall zone D are shown in Figure 2. Except for the month of September and Site-14 the model residuals lie within the 96% confidence interval (Figure 3).

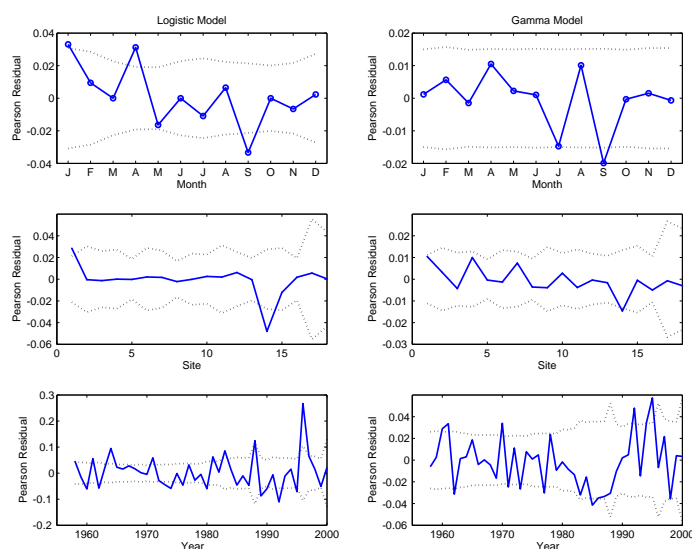


Figure 3: Pearson residuals of the occurrence model (left) and Amounts model (right) performance by month, by site and by year, over the rainfall zone D. The dotted lines indicate the 95% confidence intervals.

4.2 Projected climate change

Uganda is divided into several rainfall zones according to Basalirwa [1993] and the rainfall sites in each zone have homogeneous statistical properties. The Kyoga basin is covered by seven zones. Daily rainfall data for 30 sites was used to develop GLM models for rainfall zones D and F (Figure 2). The GLM models were later used for statistical downscaling of GCM projections. For each site 100 simulations were run for the 2020s, 2050s, and 2080s based on several GCMs outputs of the fourth assessment report of the Intergovernmental Panel on Climate Change (IPCC) [IPCC, 2007] under the A2 emission scenarios.

The ability of different GCMs to simulate historical climate was investigated by using simulation results for the 1961-1990 period for the Kyoga basin. Model performance varied by location

Table 1: Occurrence and Amounts models for rainfall zones B

| Model Predictor | | Occurrence Model Covariate Value | | Amounts Model Covariate Value |
|---|---------|-------------------------------------|---------|----------------------------------|
| Constant | | -1.699 | | 2.219 |
| Fourier sine component 1 for E | 1 | -0.509 | 1 | 0.497 |
| Fourier sine component 1 for N | 2 | 0.359 | 2 | -0.359 |
| Fourier cosine component 1 for E | 3 | 0.383 | 3 | -0.231 |
| Fourier cosine component 1 for N | 4 | 0.643 | 4 | -0.448 |
| Fourier sine component Altitude | 5 | 0.143 | 5 | -0.038 |
| Fourier cosine component Altitude | 6 | 0.173 | 6 | -0.126 |
| Monthly Indicator [Month] | Jan [7] | 0.184 | Jul [7] | 0.123 |
| | Nov [8] | 0.143 | Aug [8] | 0.096 |
| IOD West (Monthly) | 9 | 0.182 | 9 | 0.070 |
| Average Temperature (Reanalysis) | 10 | 0.038 | 10 | 0.038 |
| Relative Humidity (Reanalysis) | 11 | 0.160 | 11 | 0.048 |
| Mean Sea Level Pressure (Renalysis) | 12 | 0.035 | 12 | 0.021 |
| Daily half-year cycle, cosine component | 13 | -0.323 | 13 | -0.099 |
| Daily half-year cycle, sine component | 14 | -0.070 | 14 | -0.023 |
| Mean of I(Y[t-1]>0) | 15 | 2.428 | 15 | 0.220 |
| Mean of I(Y[t-2]>0) | 16 | 0.591 | 16 | -0.098 |
| Mean of I(Y[t-3]>0) | 17 | 0.378 | 17 | 0.068 |
| Mean of I(Y[t-4]>0) | 18 | 0.062 | 18 | -0.023 |
| 2 Way Interaction | [1 - 3] | -1.167 | [1 - 3] | 0.787 |
| | [1 - 4] | -0.335 | [1 - 4] | 0.089 |
| | [2 - 3] | -0.110 | [2 - 3] | -0.070 |
| | [2 - 4] | 0.587 | [2 - 4] | -0.124 |
| | [1 - 5] | -0.466 | [1 - 5] | 0.065 |
| | [2 - 5] | -0.173 | [2 - 5] | 0.180 |
| | [3 - 6] | 0.451 | [3 - 6] | -0.079 |
| | [4 - 5] | -0.014 | [4 - 5] | -0.002 |
| | [1 - 6] | -0.840 | [1 - 6] | 0.881 |
| | [2 - 6] | -0.158 | [2 - 6] | -0.291 |
| | [4 - 6] | 0.446 | [4 - 6] | -0.352 |
| | [7-10] | -0.020 | [7-10] | -0.174 |
| | [8-10] | -0.209 | [8-10] | -0.078 |
| | [7-15] | -0.067 | [1-15] | -0.220 |
| | [8-15] | 0.029 | [8-14] | -0.050 |
| | [10-13] | -0.016 | [7-12] | 0.003 |
| | [11-13] | 0.001 | [8-12] | 0.029 |
| | [10-14] | 0.018 | [10-13] | -0.037 |
| | [11-14] | -0.010 | [10-14] | -0.078 |
| | [13-15] | 0.295 | [11-13] | 0.016 |
| | [14-15] | -0.177 | [10-14] | 0.025 |
| | [15-16] | -1.105 | [11-14] | 0.127 |
| | [15-17] | -0.500 | [13-15] | -0.116 |
| | [11-15] | -0.130 | [13-16] | -0.049 |
| | [10-16] | -0.303 | [14-16] | -0.023 |
| | [12-15] | -0.279 | [15-16] | 0.061 |
| 'Soft' threshold for +ve values | | 0.500 | | 0.500 |
| Spatial dependence | | 7.225 | | 0.795 |
| Dispersion parameter | | | | 0.122 |

and in general GCMs have varying skills in simulating the present climate for several regions in the Kyoga basin. Although no model is better than another, inter-model variation and regional variations were expected and it is reasonable to assume higher confidence in GCM models that had the least bias (≈ 1) in simulating the historical climate. Based on this assumption, three GCM models, that is, CSIRO.MK3 [Gordon et al., 2002], MPIM.ECHAM [Roeckner and Coauthors, 2003], and UKMOHADCM3 [Gordon, 2000; Gordon et al., 2002] were selected to predict changes in observed basin water resources under the A2 emission scenarios. The other GCMs tested to estimate historical climate show that the bias in simulating the historical pattern ranges from 0.12 to 1.17 (Table 1). There was some variations in GCM precipitation estimates of historical pattern for the Mpologoma, the GFLD performing poorest (according to bias) among all GCMs.

In general all GCM tend to under-simulate the June – July precipitation amounts. The seasonal and annual changes in precipitation changes are summarised in Table 2. Average projections of precipitation vary by season. The projected annual changes in precipitation over the entire basin vary from 3 – 19 % for 2020s, -1 – 35% for 2050s and -6 – 65% for 2080s. There are substantial differences in the simulated quantities of annual precipitation change for each rainfall site. All predictions show a relative increase in annual precipitation for 2020s, 2050s, 2080s,

except for the HADCM3. For the HADCM3, precipitation predictions are highest during the 2050s. The HADCM3 generally predicts a decline in precipitation for the 2080s. The reason for the disparate predictions of the HADCM3 for the 2080s is unclear. The highest percentage increase in precipitation is observed for the MAM and SON seasons, which also correspond to the two rainfall seasons.

Table 2: [Left] Percentage change in seasonal precipitation for Mpologoma basin (Rainfall zone D and F in Figure 2); [Right] Bias from GCM experiments simulations of historical precipitation for the 1961–1990 period for Mpologoma basin.

| | | | | | |
|--------------------|-------|-------|-------|-----------------------------|------|
| CSIRO.MK3 | | | | GCM BIAS (1960-1990) | |
| Season ↓ | 2020s | 2050s | 2080s | Season ↓ | |
| DJF | 9 | -1 | 3 | DJF | 0.91 |
| MAM | -4 | 0 | 34 | MAM | 1.00 |
| JJA | -2 | -2 | -7 | JJA | 0.61 |
| SON | -11 | -2 | 51 | SON | 0.88 |
| ANNUAL | 3 | -1 | 26 | ANNUAL | 0.88 |
| MPIM.ECHAM | | | | GCM BIAS (1960-1990) | |
| Season ↓ | 2020s | 2050s | 2080s | Season ↓ | |
| DJF | 12 | 7 | 4 | DJF | 1.03 |
| MAM | 41 | 69 | 116 | MAM | 1.17 |
| JJA | -10 | -10 | -12 | JJA | 0.52 |
| SON | 14 | 39 | 87 | SON | 1.13 |
| ANNUAL | 19 | 35 | 65 | ANNUAL | 1.02 |
| UKMO.HADCM3 | | | | GCM BIAS (1960-1990) | |
| Season ↓ | 2020s | 2050s | 2080s | Season ↓ | |
| DJF | -7 | -9 | 0 | DJF | 1.61 |
| MAM | 27 | 56 | -19 | MAM | 1.18 |
| JJA | -3 | -6 | -1 | JJA | 1.14 |
| ANNUAL | 19 | 36 | -6 | ANNUAL | 1.16 |

4.3 Sensitivity of hydrological variables

Daily hydrological model runs were made using an existing/calibrated SWAT model for the Mpologoma basin [Kigobe, 2009]. Calibration statistics for the Mpologoma model are shown Table 3. Daily simulations were run for the current period (1960 - 1990) - referred to as the baseline period, and for the future periods, i.e (2010 – 2040, 2040 – 2070 and 2070 – 2100) - referred to as the climate projection periods. Simulated variable were aggregated to give monthly statistics of water resources variables (including stream flow, evapotranspiration, soil water, deep aquifer recharge and water yield). The scope of this paper is limited to stream flows and evapotranspiration alone.

Sensitivity of Evapotranspiration. Evapotranspiration rates are controlled by several variables including the the available water and energy. A temperature increase leads to higher energy available for evapotranspiration. Although a warmer atmosphere can hold more water, the actual changes in evapotranspiration will depend on the humidity levels and the wind patterns. Due to data limitations, using the Hargreaves method, the simulations for the Mpologoma basin suggest that annual estimates of evapotranspiration are predicted to increase with increase in temperature and precipitation. The projected increase in evapotranspiration is on average 6 - 20% for the 2020s and 2050s, and about 10 - 25% for the 2080s.

Sensitivity of Stream flows. The sensitivity of the average annual runoff using the calibrated hydrological model is shown in Figure 4. This was obtained using an ensemble of several precipitation simulations for three GCM projections for the 2020s, 2050s and 2080s and multiple model parameter sets. On a monthly scale, the associated prediction uncertainty estimates by the different GCM models generally suggest higher uncertainty for high flow simulations (Figure 4). The projected changes in stream flows differ with GCMs. Simulated stream flows show a consistent increase in stream flow volumes especially for April to July and October to November. For the 2080 the HADCM predicts the least increase in stream flows.

To have an indication of water resource availability in the Mpologoma basin, the change in mean annual runoff was examined. Simulations show a remarkable increase in stream flow and stream flow variance for the 2050s and 2080s (Table 4). The results suggest that the daily mean flow, variance of daily flows and skewness of daily flows increases. The variance shows a slight increase for the 2020 periods and a great increase for the 2050s and 2080s. The skewness tends to decrease for simulated flows at Mpologoma suggesting a reduction in the frequency of extreme events.

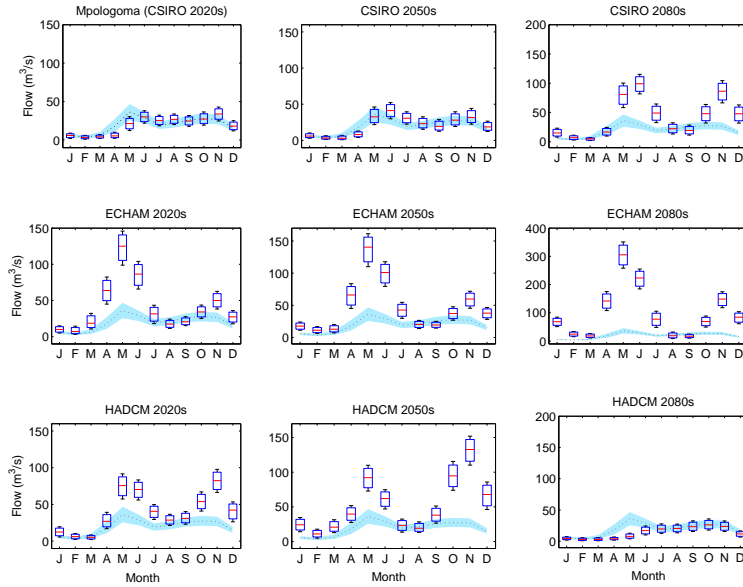


Figure 4: Simulated mean monthly stream flow at Mpologoma for the 2020s, 2050s, 2080s. The box plots show the spread of simulation ensembles at the 5%, 25%, 50%, 75% and 95% percentiles. The shaded area shows the 95PPU for the simulated flows for 1960 – 1990 period.

Table 3: Calibration statistics for Mpologoma basin using apriori parameters. The *p-factor* is the percentage of observations bracketed by the 95% prediction uncertainty. The *d-factor* is the average thickness of the 95PPU band divided by the standard deviation of the measured data; *NSE* is Nash Sutcliffe efficiency, and *bR²* is an objective function where *b* is the slope of the regression line between measured and simulated variable and *R²* is the coefficient of determination.

| Flow station (location) | Uncertainty Estimate | | Objective Function | | | |
|-------------------------|----------------------|-----------------|----------------------|------------|------------|-----------------------|
| | <i>p-factor</i> | <i>d-factor</i> | <i>R²</i> | <i>NSE</i> | <i>MSE</i> | <i>br²</i> |
| apriori parameter set | 0.50 | 1.53 | 0.38 | 0.1 | 373 | 0.17 |
| calibration period | 0.55 | 0.86 | 0.60 | 0.65 | 291 | 0.43 |
| validation period | 0.65 | 0.65 | 0.47 | 0.45 | 138 | 0.19 |

5 CONCLUSIONS AND DISCUSSIONS

This paper demonstrates the use of GLM models in downscaling projections of local and regional rainfall in the Mpologoma basin within the Upper Nile using the A2 emission scenario. The biases across the different GCMs give a general indication of the simulation strengths and weaknesses, when using different GCMs to simulate the historical climate. GCMs are still limited in simulating

Table 4: Comparison of basic annual statistics (mean, variance and skewness) of daily stream flow for Mpologoma basin. The values are averages for CSIRO, ECHAM and HADCM models at the 50th percentile.

| Simulation Period | Mean (m ³ /s) | St.Dev (m ³ /s) | Skewness |
|-------------------|--------------------------|----------------------------|----------|
| 1960 – 1990 | 10.7 | 7.4 | 2.0 |
| 2020s | 12.1 | 8.7 | 1.8 |
| 2050s | 13.3 | 9.2 | 1.7 |
| 2080s | 17.5 | 13.5 | 1.4 |

the chaotic nature of climate and additional work is required to refine GCM models for climate prediction [Dessai et al., 2009; Harrison Stainforth, 2009].

The sensitivity of the Mpologoma basin to changes in climate has been investigated using the SWAT model, a semi-distributed hydrological model. This was achieved by driving the hydrological model with projected temperature and downscaled daily precipitation sequences for three GCM projections for the A2 scenario. Simulated evapotranspiration rates and stream flow suggest major shifts in hydrological regimes, with a tendency to result in significantly higher monthly average flows and higher evapotranspiration rates. This may subsequently lead to variation in the timing of floods and droughts. Using the 95% prediction uncertainty, the results generally suggest higher uncertainty for high flows. The simulation results presented suggest that even with a high increase in precipitation, excessive evapotranspiration might lead to a decline in other hydrological variables such as soil moisture. This may pose serious concerns for food security and water resource sustainability. Therefore, adaptation strategies in and around the Mpologoma basin have to be developed in the context of other regional challenges that might contribute to water conflicts.

6 ACKNOWLEDGMENT

This study was funded by ACCION projects. The stream flow series and the climate data sets were kindly provided by the Directorate of Water Development (DWD), Ministry of Water and Environment, Uganda. The authors would also like to thank the staff of UNESCO-IHE for providing the required simulation facilities.

REFERENCES

- Abbaspour, K. C. Modelling hydrology and water quality in the pre-alpine/alpine Thur watershed using SWAT. *Journal of Hydrology*, 333(2-4):413, 2007.
- Abbaspour, K. C., J. Yang, P. Reichert, M. Vejdani, S. Haghighat, and R. Srinivasan. SWAT Calibration and Uncertainty Programs - A User Manual, 2008.
- Arnold, J. G. SWAT 2000: current capabilities and research opportunities in applied watershed modelling. *Hydrological Processes*, 19(3):563, 2005.
- Arnold, J. G., R. Srinivasan, R. S. Muttiah, and J. R. Williams. Large area hydrologic modeling and assessment Part I: Model development. *Journal - American Water Resources Association*, 34(1):73–89, 1998.
- Basalirwa, C. P. K. The design of a regional minimum raingauge network. *International journal of water resources development*, 9(4):411, 1993.
- Chandler, R. GLIMCLIM: Generalized linear modelling for daily climate time series. Technical report, Available at <http://www.ucl.ac.uk/stats/research/>, 2002.
- Chandler, R. On the use of generalized linear models for interpreting climate variability. *Environmetrics*, 16(7):699–715, 2005.
- Chandler, R. and H. S. Wheeler. Analysis of rainfall variability using generalized linear models: A case study from the west of Ireland. *Water Resour. Res*, 38(10):1192, 2002.

- Chandler, R. GLIMCLIM: Generalized linear modelling for daily climate time series: Software and User guide, 2006.
- Conway, D. and M. Hulme. Recent fluctuations in precipitation and runoff over the Nile sub-basins and their impact on Main Nile discharge. *Climatic Change*, 25(2):127–151, 1993.
- Fowler, H. and C. Kilsby. Using regional climate model data to simulate historical and future river flows in northwest England. *Climatic Change*, 80(3):337–367, 2007.
- Gassman, P., M. Reyes, C. Green, and J. Arnold. The Soil and Water Assessment Tool: Historical Development, Applications, and Future Research Directions, 2007.
- Gordon, C. The simulation of SST, sea ice extents and ocean heat transports in a version of the Hadley Centre coupled model without flux adjustments. *Climate Dynamics*, 16(2):147, 2000.
- Gordon, H., L. Rotstayn, J. McGregor, M. Dix, E. Kowalczyk, S. O'Farrell, L. Waterman, A. Hirst, S. Wilson, M. Collier, I. Watterson, and T. Elliott. The CSIRO MK3 climate system model. CSIRO Marine and Atmospheric Research Technical Report 60 <http://www.cmar.csiro.au/e-print/open/gordon2002a.pdf> 130pp. 2002.
- Hulme, M. *Using a climate scenario generator for vulnerability and adaptation assessments: MAGICC and SCENGEN Version 2.4 Workbook*. Climatic Research Unit, Norwich, UK, 2000.
- Hulme, M., R. Doherty, T. Ngara, and N. New. Global warming and African climate change: a reassessment. In Low, P. S., editor, *Climate Change and Africa*. Cambridge University Press, Cambridge, 2005.
- IPCC. *Climate Change 2007: The Physical Scientific Basis*. Cambridge University Press, Cambridge, United Kingdom and New York, NY, USA, 2007.
- Kigobe, M. *Modelling the effects of land use change and climate variability on the hydrology of the Upper Nile*. PhD thesis, Imperial College London, 2009.
- Neitsch, S., A. J.G., J. Williams, S. Temple Texas, USA: ARS Grassland, W. R. Service, and T. B. R. Center. Soil and Water Assessment Tool. User's Manual Version 2000, 2000.
- Roeckner, E. and Coauthors. The atmospheric general circulation model ECHAM5. Part I: Model description. Technical report, Max Planck Institute for Meteorology, 2003.
- SCS, S. C. S. *Section 4: Hydrology, National Engineering Handbook*. United States Department of Agriculture, Washington, D.C., USA, 1972.
- Stern, R. and R. Coe. A model fitting analysis of daily rainfall data. *Journal of the Royal Statistical Society*, A147:1–34, 1984.
- Yang, C., R. E. Chandler, V. S. Isham, C. Annoni, and H. S. Wheeler. Simulation and downscaling models for potential evaporation. *Journal of Hydrology*, 302(1-4):239–254, 2005.